

# Testing mutual exclusivity of ETS rearranged prostate cancer

Maria A Svensson<sup>1,2</sup>, Christopher J LaFargue<sup>1</sup>, Theresa Y MacDonald<sup>1</sup>, Dorothee Pflueger<sup>1</sup>, Naoki Kitabayashi<sup>1</sup>, Ashley M Santa-Cruz<sup>3</sup>, Karl E Garsha<sup>3</sup>, Ubaradka G Sathyanarayana<sup>3</sup>, Janice P Riley<sup>3</sup>, Chol S Yun<sup>3</sup>, Dea Nagy<sup>3</sup>, Jerry W Kosmeder<sup>3</sup>, Gary A Pestano<sup>3</sup>, Ashutosh K Tewari<sup>4</sup>, Francesca Demichelis<sup>1,5</sup> and Mark A Rubin<sup>1</sup>

Prostate cancer is a clinically heterogeneous and multifocal disease. More than 80% of patients with prostate cancer harbor multiple geographically discrete cancer foci at the time of diagnosis. Emerging data suggest that these foci are molecularly distinct consistent with the hypothesis that they arise as independent clones. One of the strongest arguments is the heterogeneity observed in the status of E26 transformation specific (ETS) rearrangements between discrete tumor foci. The clonal evolution of individual prostate cancer foci based on recent studies demonstrates intertumoral heterogeneity with intratumoral homogeneity. The issue of multifocality and interfocal heterogeneity is important and has not been fully elucidated due to lack of the systematic evaluation of ETS rearrangements in multiple tumor sites. The current study investigates the frequency of multiple gene rearrangements within the same focus and between different cancer foci. Fluorescence *in situ* hybridization (FISH) assays were designed to detect the four most common recurrent ETS gene rearrangements. In a cohort of 88 men with localized prostate cancer, we found *ERG*, *ETV1*, and *ETV5* rearrangements in 51% (44/86), 6% (5/85), and 1% (1/86), respectively. None of the cases demonstrated *ETV4* rearrangements. Mutual exclusiveness of ETS rearrangements was observed in the majority of cases; however, in six cases, we discovered multiple ETS or 5' fusion partner rearrangements within the same tumor focus. In conclusion, we provide further evidence for prostate cancer tumor heterogeneity with the identification of multiple concurrent gene rearrangements.

*Laboratory Investigation* (2011) 91, 404–412; doi:10.1038/labinvest.2010.179; published online 25 October 2010

**KEYWORDS:** ETS (E26 transformation specific) rearrangements; *TMPRSS2-ERG*; heterogeneity; prostate cancer

Prostate cancer is a clinically heterogeneous and multifocal disease.<sup>1,2</sup> More than 80% of patients with prostate cancer harbor multiple geographically discrete cancer foci at the time of diagnosis.<sup>3</sup> Emerging molecular data suggest that these foci are molecularly distinct consistent with them arising as independent clones.<sup>4</sup> One of the strongest pieces of data is the heterogeneity observed in the status of E26 transformation specific (ETS) transcription factors rearrangements between different foci. ETS rearrangements occur early in the development of prostate cancer.<sup>5</sup> Although a number of rearrangements involving different ETS genes and different 5' fusion partners have been described,<sup>6</sup> the fusion of *ERG* with the androgen-regulated *TMPRSS2* gene is the most common recurrent lesion in prostate cancer,

occurring in ~45% of screened prostate cancers.<sup>7</sup> The clonal evolution of individual prostate cancer foci based on recent studies demonstrates intertumoral heterogeneity with intratumoral homogeneity.<sup>8–10</sup> This supports the view that these tumors developed separately or diverged molecularly at an early time point.<sup>8,10,11</sup> When studying metastases of men who died of castration-resistant prostate cancer, Mehra *et al*<sup>11</sup> demonstrated the clonal expansion of tumors to metastatic sites. Two recent studies further support this concept by demonstrating that the metastases are more consistent with clones than the heterogeneous population of tumor cells.<sup>12,13</sup>

The initial observation that ETS rearrangements are mutually exclusive supports the hypothesis that the molecular

<sup>1</sup>Department of Pathology and Laboratory Medicine, Weill Cornell Medical College, New York, NY, USA; <sup>2</sup>Department of Laboratory Medicine, University Hospital of Örebro, Örebro, Sweden; <sup>3</sup>Ventana, a Member of the Roche Group, Tucson, AZ, USA; <sup>4</sup>Department of Urology, Weill Cornell Medical College, New York, NY, USA and <sup>5</sup>Institute for Computational Biomedicine, Weill Cornell Medical College, New York, NY, USA  
Correspondence: Dr MA Rubin, MD, Department of Pathology and Laboratory Medicine, Weill Cornell Medical College, 1300 York Avenue Room C 410-A, New York, NY 10065, USA.

E-mail: rubinma@med.cornell.edu

Received 7 May 2010; revised 2 September 2010; accepted 2 September 2010

lesion is a driving alteration in each cancer focus.<sup>14</sup> However, Clark *et al*<sup>10</sup> demonstrated an example of two ETS gene rearrangements (ie *ERG* and *ETV1*) involving two separate tumor foci from the same patient. Han *et al*<sup>15</sup> screened for 27 ETS genes and all known 5' fusion partners in a cohort of 110 tumors from a prostatectomy series captured on a tissue microarray (TMA). Besides identifying novel fusions including *SLC45A3-ERG* and *DDX5-ETV4*, they further identified three cases with *TMPRSS2-ERG* fusion and an additional alteration with either the 5' or 3' end of another ETS gene being deleted. This finding suggests that the rule of mutual exclusiveness of ETS rearrangements may have exceptions. Therefore, in order to test the rule of mutual exclusiveness, we present a detailed analysis of four recurrent ETS rearrangements in a US prostatectomy cohort.

## MATERIALS AND METHODS

### Cohort Description

The study cohort is comprised of 88 patients (mean age 63.2 years) who underwent radical prostatectomy at Weill Cornell Medical College (New York, NY, USA) as a monotherapy. The pathological stages ranged from organ confined to cases with extraprostatic tumor extension. The prostate gland was evaluated for discrete tumor foci. A prostate cancer sample was considered multifocal if tumor nodules were identified on contralateral sides of the gland. Ipsilateral tumor nodules were defined as separated by a minimum of 3 mm from the nearest tumor nodule in any single section or by a minimum of 4 mm from the closest nodule on the adjacent section above or below.<sup>2,16</sup> Tumor maps were generated by tracking each section according to the pathology report and reconstructing them in a whole-mount manner. Primary, secondary, tertiary, and quaternary tumor foci from the prostate were designated in decreasing order based on tumor diameter (cm).

### TMA Construction

Histologic examination of all tumor foci was performed by the study pathologists. The pathologists circled representative areas within each focus from which three 0.6 mm cancer cores were sampled for TMA construction. This resulted in a TMA with representative tumor samples from each histologically discrete tumor focus identified for all of the prostate cancer cases included in the study. The study was approved by the Weill Cornell Medical College IRB.

### Assessment of Gene Rearrangement Status by Dual-Color Interphase Fluorescence *In Situ* Hybridization

Four-micron thick TMA sections were used for interphase fluorescence *in situ* hybridization (FISH). Based on the systematic evaluation of 27 ETS rearrangements by Han *et al*,<sup>15</sup> we selected four ETS genes for evaluation: *ERG*, *ETV1*, *ETV4*, and *ETV5*. We also chose four recurrent 5' fusion partners: *TMPRSS2*, *SLC45A3*, *NDRG1*, and *Herv-K22q11.23*. The following centromeric/telomeric BAC clones were used to

assess for rearrangement status: *ERG* (RP11-24A11 and RP11-372O17), *ETV1* (RP11-661L15 and RP11-79G16), *ETV5* (RP11-480B15 and RP11-822O23), *ETV4* (CTP-3215I16 and RP11-147C10), *TMPRSS2* (RP11-35C4 and RP11-120C17), *SLC45A3* (RP11-249H15 and RP11-131E5), *NDRG1* (RP11-185E14 and RP11-1145H17), and *Herv-K22q11.23* (RP11-61N10 and RP11-71G19). Break apart dual-color interphase FISH assay was performed as previously described,<sup>5,14,17</sup> as an approach to systematically identify putative rearrangements. This FISH assay enables us to distinguish between two different rearrangement mechanisms, rearrangement through insertion and rearrangement through deletion as previously described. A nucleus without a rearrangement demonstrates two pairs of juxtaposed red and green signals (mostly forming two yellow signals). A nucleus with rearrangement through insertion shows the split of one red–green (yellow) signal pair, resulting in a single red and green signal for the rearranged allele, and a still combined (yellow) signal for the non-rearranged allele in each nucleus. Finally, a nucleus with a rearrangement through deletion shows one juxtaposed red–green signal pair (yellow) for the non-rearranged allele, and a single red signal for the allele involved in the rearrangement. When finding cases with multiple 5' or 3' rearrangements in a case on the TMA, we went back to the tissue block that was used to construct the TMA and performed fusion FISH to assess for gene fusions, using differently labeled probes for each gene of interest. When a fusion occurs, the signal patterns is opposite from the break apart assay. In a fusion assay, the red–green signal pair (yellow) is representing the two fused genes, whereas the separate red and green signals represent the genes that are not fused. The following probe combinations were used for fusion FISH: RP11-131E5 and RP11-24A11 (*SLC45A3-ERG* fusion), RP11-131E5 and RP11-692L4 (*SLC45A3-ETV1* fusion), RP11-35C4 and RP11-692L4 (*TMPRSS2-ETV1* fusion), RP11-185E14 and RP11-372O17 (*NDRG1-ERG* fusion), and RP11-131E5 and RP11-480B15 (*SLC45A3-ETV5* fusion). For each case, at least 100 cancer nuclei were assessed, and a case was considered to be rearranged if at least 20% of the nuclei assessed harbored a rearrangement. With a minimum of 20% rearranged nuclei as a cutoff for calling a case positive, we believe that we can be certain that we are seeing an actual rearrangement event and not an event due to artifacts that can be caused by the thickness of the tissue section or overlapping nuclei. Percentages of rearrangements were evaluated by considering a case positive if at least one focus was positive.

### Four-Color Automated *In Situ* Hybridization

To be able to confirm co-occurring 5' gene rearrangements within one nucleus, we applied the new four-color Quantum dot (QD) technology *in situ* hybridization. With this technique, it is possible to multiplex the FISH assay by using four differently labeled probes (QD) instead of the conventional FISH, which have two differently labeled probes. All steps

from deparaffinization of slides through detection were conducted on the BenchMark<sup>®</sup>XT automated slide processing system (Ventana Medical Systems, Tucson, AZ, USA). Unless otherwise, all reagents used in the automated four-color *in situ* hybridization protocol are from Ventana. Briefly, slides were deparaffinized using a combination of heat (65 °C, 25 min) and a mild detergent (EZ-Prep, Ventana) at 76 °C with eight washes for 1 min each. Antigen retrieval was conducted in the presence of heat (90 °C, 8 min) and a serine protease (0.02 CU/ml, 12 min). Genomic DNA was denatured online at 95 °C for 5 min, followed by probe hybridization for 8 h at 52 °C in Hybrizol. All four probes were simultaneously applied as a cocktail at 8 µg each per slide. Human placental DNA (200 µg per slide) was used to block repetitive DNA sequences. BAC probes for 5' and 3' NDRG1, and 5' and 3' TMPRSS2 were labeled with the respective dNTP haptens using random priming as described previously.<sup>18</sup> Specifically, 5' NDRG1 was labeled with dUTP biotin (Roche, Penzberg, Germany), 3' NDRG1 with dUTP TS (thiazole sulfonamide) (Ventana), 5' TMPRSS2 with amino dUTP DNP (Ventana), and 3' TMPRSS2 with dUTP DIG (Roche). Detection was conducted online as a part of the Benchmark<sup>®</sup>XT protocol with sAV QD625 (Life Technologies, OR, USA), mouse monoclonal anti-TS (clone 13A06-01E11, Ventana) conjugated to QD605, mouse monoclonal anti-DNP (clone 1C7-1C7, Ventana) conjugated to QD655, and with mouse monoclonal anti-DIG (clone 1-171-256, Roche) conjugated to QD565. All antibody conjugations were conducted using 30n PEGylated QD (Life Technologies) and purified monoclonal antibodies.<sup>19</sup> DAPI (Ventana) was also applied online to counter-stain nuclei for imaging.

#### QD FISH image capture and analysis

Spectral image cubes containing high-resolution wavelength intensity information at each pixel were captured using a modified SpectraView<sup>™</sup> acquisition and analysis system (ASI; Applied Spectral Imaging, Israel). The modified system comprises a computer workstation, fluorescent microscope (Olympus BX61), a light-guide coupled, and stabilized metal halide excitation source (Exfo Exacte, Exfo, Ontario, CA, USA), with spectral output from an interferometer optical head to a Sony ICX285 digital CCD.<sup>20–23</sup> The excitation/emission filters for spectral imaging (Semrock, USA) were as follows: 377 nm center wavelength with 50 nm bandwidth for excitation; dichroic beamsplitter with reflection band below 410 nm, and a long pass filter with deep blocking transition at 409 nm. All spectral image cubes were captured with a × 40 plan-fluor objective (numerical aperture 0.75) and × 1 c-mount.

Data were gathered through a series of 100 ms exposures to build the interferometric image cube for spectral processing. The wavelength range represented by image cubes captured under these conditions covered the visible wavelengths between 410 and 900 nm at a 10-nm wavelength sampling resolution. Spectral unmixing to separate signals corresponding to tissue autofluorescence, DAPI, QD 565, QD 605, QD 625, and QD 655 was conducted using the appropriate reference spectra and linear unmixing algorithms<sup>24</sup> implemented in SpectraView<sup>™</sup> spectral data analysis software (ASI). The distinctive narrow Gaussian wavelength distribution and discrete peak locations of the QD emission spectra enabled reliable separation of the individual probe signals. The individual monochrome FISH signal intensity layers were colorized and merged to provide overlay images for visualization of relative probe localizations using Image-Pro Plus image analysis and measurement software (Media Cybernetics, USA). For the automated *in situ* hybridization, the same evaluation criteria and cutoff were used as for the standard FISH assay (ie manual assessment of a minimum of 100 nuclei/case with a rearrangement occurrence in a minimum of 20% of the assessed nuclei to be called rearrangement positive).

#### Statistical Analysis

Within the set of cases with *ERG*, *TMPRSS2*, and *SLC45A3* rearrangements, we investigated for significant association, using Pearson  $\chi^2$  test, between the different rearrangements with Gleason grade and pathological stage. For the cases with *ERG* rearrangements, we further distinguished between the two types of rearrangement mechanisms (ie rearrangement through insertion or deletion). A two-tailed *P*-value of  $\leq 0.05$  was considered significant. Given the number of samples screened for rearrangement ( $n = 88$ ), this study is powered to detect rearrangements with incidence of 3.5% ( $P = 0.05$ ). Therefore, there is uncertainty when we found percent incidence below 3.5%.

## RESULTS

### Frequency of Three Common ETS Gene Rearrangements

We evaluated 88 cases of localized prostate cancer for rearrangements of the four recurrent ETS genes (Figure 1). *ERG*, *ETV1*, and *ETV5* were rearranged in 51% (44/86), 6% (5/85), and 1% (1/86) of the cases, respectively. None of the cases demonstrated rearrangement for *ETV4* (Table 1). *ERG* rearrangement through insertion was seen in 52% (23/44), rearrangement through deletion in 39% (17/44). Interestingly, four cases with multiple tumor foci demonstrated rearrangement through insertion in one focus and rearrangement through deletion in the other focus (Figure 2).

**Figure 1** Summary matrix of 5' gene fusion partners and ETS genes rearrangements investigated, sorted to show the rearranged cases first. Case number, focus-specific subnumber, Gleason grade (pertaining to the core), and stage are indicated on the left. The subnumbers represent the different tumor foci of the case. Color legend signifies respective aberration and availability. Rearrangement through insertion (T), rearrangement through deletion (T + D), copy number increase (CNI).

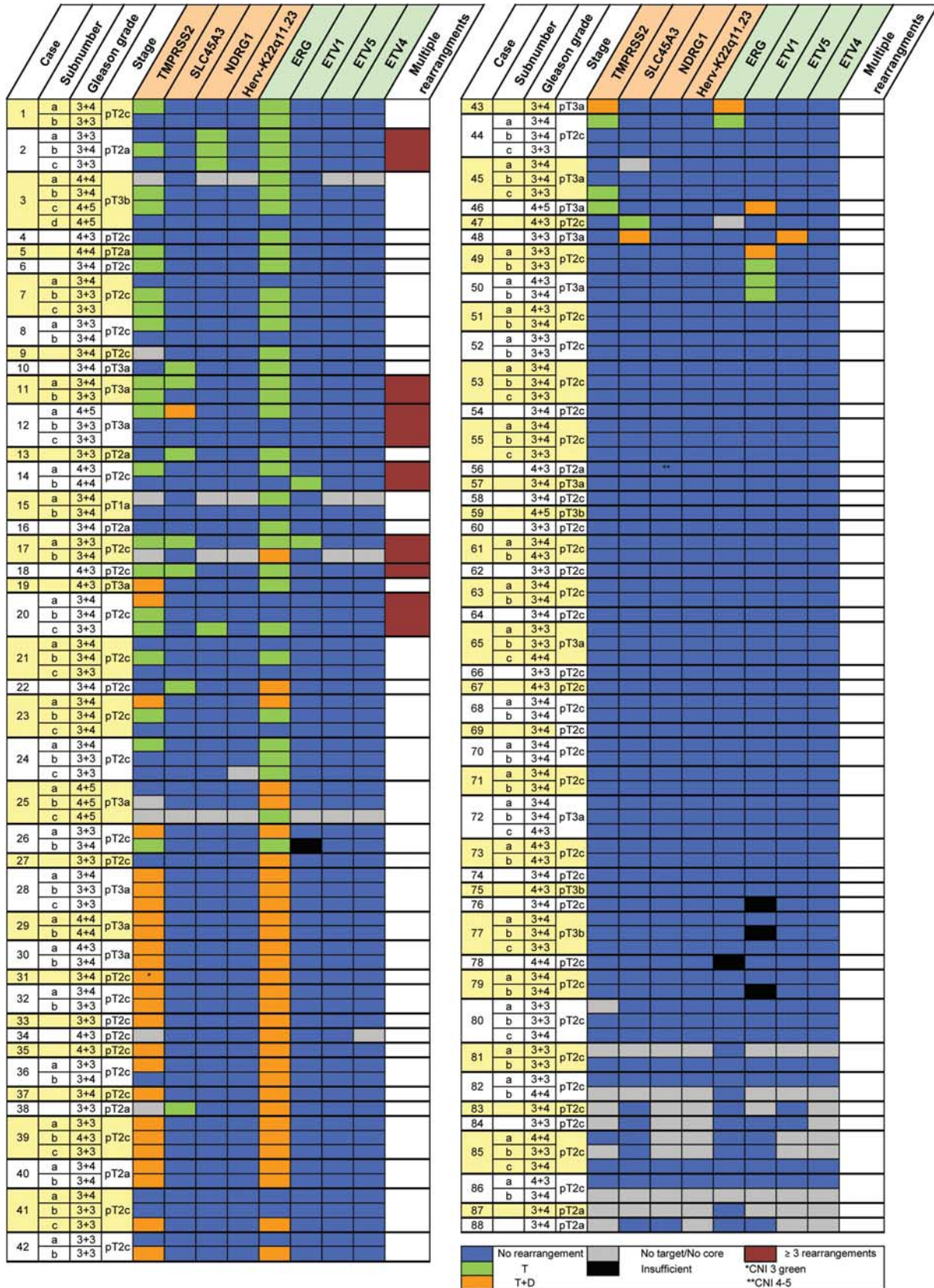


**Table 1** Rearrangement frequencies are given in percentages (number of rearranged cases/evaluable cases), as shown in Figure 1

	5' Gene fusion partners				ETS genes			
	TMPRSS2	SLC45A3	NDRG1	Herv-K22q11.23	ERG	ETV1	ETV5	ETV4
Rearranged cases	43.2% (35/81)	11.6% (10/86)	2.4% (2/85)	0.0% (0/84)	51.2% (44/86)	5.9% (5/85)	1.2% (1/86)	0.0% (0/83)

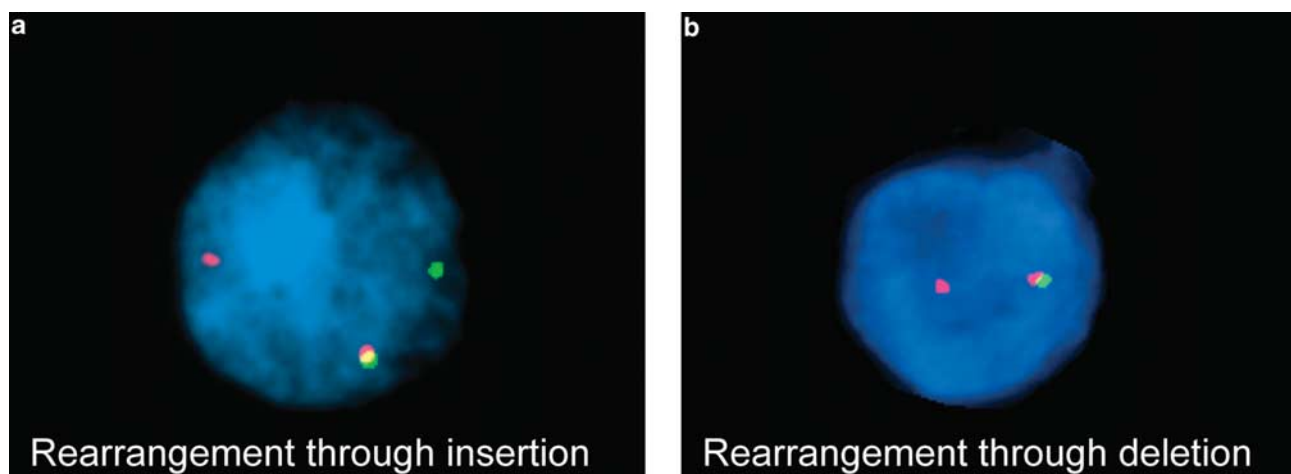


**Figure 2** Representative example showing FISH images with gene rearrangement (here *ERG*) with different rearrangement mechanisms, (a) rearrangement through insertion (b) rearrangement through deletion, in separate tumor foci in one case.

The rearrangement frequencies of the most common 5' fusion partners *TMPRSS2* and *SLC45A3* were 43% (35/81) and 12% (10/86), respectively. None of the cases demonstrated rearrangement for *Herv-K22q11.23* (Table 1). We also found the novel 5' fusion partner *NDRG1*<sup>25</sup> to be rearranged in 2% (2/85) of the cases. Before starting with the FISH assessments, we set a cutoff of a minimum of 20% rearranged nuclei to call a case rearrangement positive. However, after evaluating the cohort for the different gene rearrangements, we found that in 95% of the cases, the rearrangements were seen in >50% of the evaluated nuclei. Based on our power calculations, the true incidence of the genes reported in this study as not being rearranged can vary between 0 and 3.5% in the population. We did not observe any statistically significant associations between *TMPRSS2-ERG* and *SLC45A3-ERG* rearrangements with Gleason grade or pathological stage. On a subset of cases (37/88), we performed *TMPRSS2-ERG* fusion transcript analysis with qRT-PCR and found that 35/37 cases were in agreement with our FISH results (data not shown). The two discrepant cases may be due to sampling where the tissue cored for PCR was not directly adjacent to the tissue used in the TMA. Alternatively, the PCR primers used do not capture all *TMPRSS2-ERG* isoforms.

### ETS Rearrangements in Cases of Multifocal Prostate Cancer

Fifty-five percent (48/88) of the prostate cancer cases had multiple, discrete tumor foci. We were able to assess 44/48 of

the cases for multifocal heterogeneity in all the genes investigated in this study. Interfocal homogeneity was observed in 24/44 cases (Figure 1), with 15 cases negative for all gene rearrangements. Nine cases were positive for the same gene rearrangements throughout all tumor foci. Of these nine cases, six were positive for *TMPRSS2-ERG* rearrangement, all through deletion mechanism. One case (#26) showed *TMPRSS2-ERG* rearrangement with one focus rearranged through deletion and the other focus rearranged through insertion for both genes, respectively. Three cases showed *ETV1* rearrangement without any co-occurring rearrangement of the 5' partners screened in this study, suggesting another 5' partner. One of these cases (#49) harbored both rearrangement through insertion in one focus and rearrangement through deletion in the other. The remaining 20 cases displayed interfocal heterogeneity.

From 88 cases, we observed *TMPRSS2-ERG* rearrangement in at least one focus in 33 cases. Twenty-six of these cases displayed a mutually exclusive pattern for only *TMPRSS2* and *ERG* rearrangement, with 35% (9/26) being rearranged through insertion, 54% (14/26) through deletion, and 12% (3/26) showing both rearrangement mechanisms. The remaining seven cases showed at least one more gene rearranged, in addition to *TMPRSS2* and *ERG* (Table 2). This co-occurrence of multiple gene rearrangements was seen in a subset of the same cells in the tumor focus (Figure 3). Five of these seven cases had a second 5' gene rearrangement along with the ETS gene rearrangement in the same tumor focus

(Figure 1). Three of the five cases showed co-occurring rearrangements of 5' partners *TMPRSS2* and *SLC45A3* along with *ERG* rearrangement. *SLC45A3-ERG* fusion could not be confirmed in these cases by FISH, suggesting *TMPRSS2-ERG* fusion and a different 3' fusion partner to *SLC45A3*. Two cases harbored *TMPRSS2* and *NDRG1* rearrangement with

co-occurring *ERG* rearrangement. In case #20, *NDRG1-ERG* fusion could be confirmed by FISH. Case #2 was earlier confirmed as a *NDRG1-ERG* fusion by RT-PCR in a study by Pflueger *et al*<sup>25</sup>. One case (#17) showed two ETS genes (ie *ERG* and *ETV1*) and two 5' partners (ie *TMPRSS2* and *SLC45A3*) to be rearranged in the same focus, but we could not confirm that two fusions were present in the same focus using FISH fusions assays (Figure 4). The last case (#14) demonstrated multiple rearrangements in different foci of the prostate. Interestingly, all seven cases harboring multiple rearrangements showed *ERG* rearrangement through insertion. We implemented a novel assay using four-color *in situ* hybridization to demonstrate the simultaneous rearrangements in the same cells of the tumor. For this approach, we used a case (#20) harboring *TMPRSS2*, *NDRG1*, and *ERG* rearrangements to confirm simultaneous rearrangements (Figure 3). No association was observed between harboring

**Table 2 Event summary of co-occurring gene rearrangements**

	ERG	ETV1	ETV5	ETV4	Total number of events
<i>TMPRSS2</i>	35	3	0	0	38
<i>SLC45A3</i>	9	0	1	0	10
<i>NDRG1</i>	2	1	0	0	3
Total number of events	46	4	1	0	

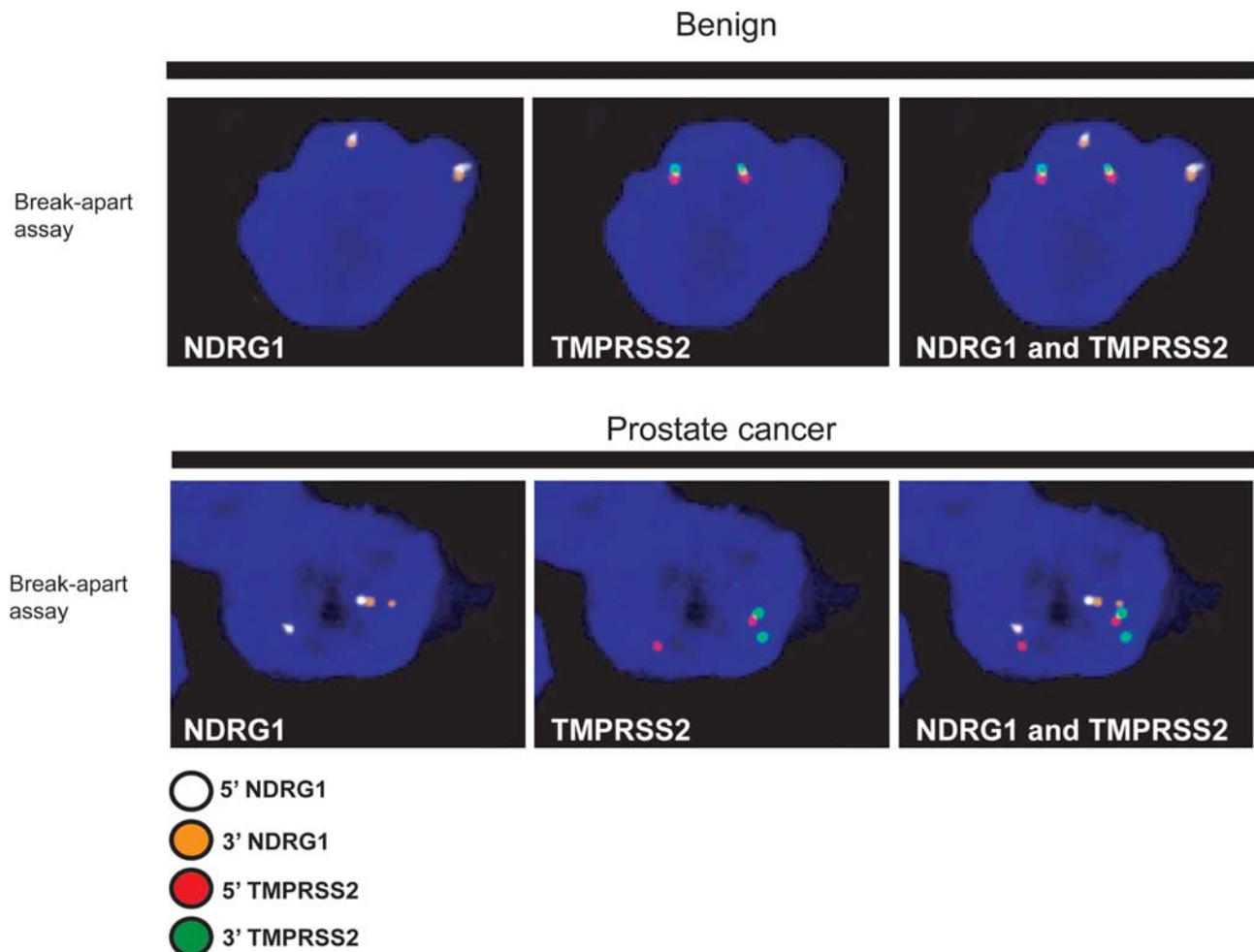


**Figure 3** Simultaneous rearrangement of *TMPRSS2* and *NDRG1* in the same cancer nucleus demonstrated by four-color FISH. By using four differently labeled probes, we are able to show simultaneous rearrangements of two 5' gene fusion partners within the same nucleus. Top panel shows a benign nucleus. The first two images from the left show no rearrangement of *NDRG1* and *TMPRSS2*, respectively. Top right image shows the merged signals of *NDRG1* and *TMPRSS2* in the same nucleus. Bottom panel shows a prostate cancer nucleus with *NDRG1* (left) and *TMPRSS2* (middle) rearrangement. Bottom right image shows the merged image of the two gene rearrangements within the same nucleus. This case (#20) also harbors *ERG* rearrangement (not shown).

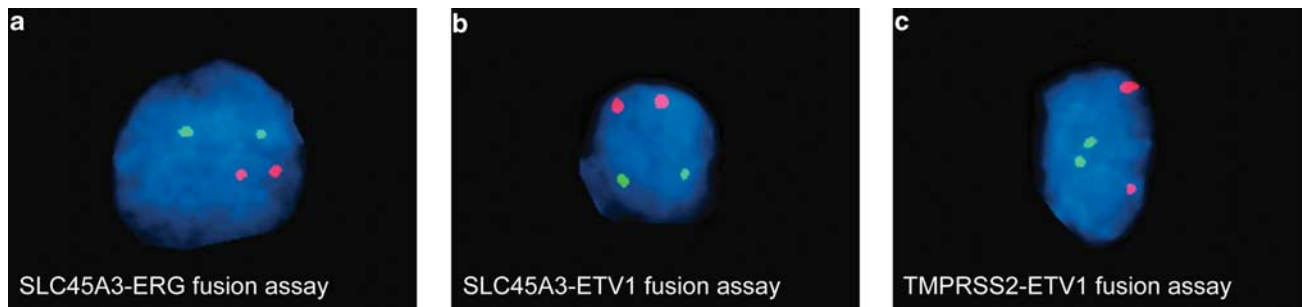


**Figure 4** Co-occurring rearrangements of the two ETS genes. In case #17, we see co-occurring rearrangement of *ERG* and *ETV1* (red-labeled FISH probe) and two 5' gene partners, *TMPRSS2* and *SLC45A3* (green-labeled FISH probe). All rearrangements were through insertion mechanism. Fusion FISH was performed but could not identify multiple fusions within the focus. Fusion assay with *SLC45A3-ERG* (a), *SLC45A3-ETV1* (b), and finally *TMPRSS2-ETV1* (c).

multiple rearrangements and Gleason grade or stage. Similarly, we did not observe association between intraindividual heterogeneity in terms of rearrangement status and Gleason grade or stage.

## DISCUSSION

The original observation that ETS fusions are mutually exclusive<sup>14</sup> holds true within an individual tumor focus in the majority of cases tested. This study confirms the observation made by Clark *et al*<sup>10</sup> that more than one ETS rearrangement can exist in a prostate gland. The current study also systematically demonstrates that ETS rearrangements may serve as clonal markers of tumors when present. However, mutual exclusivity of ETS rearrangements does have exceptions. We observed that 8% of the cases harbored a *TMPRSS2-ERG* gene rearrangement plus an additional gene rearrangement within the same focus in six out of seven cases. In these six cases, we could confirm multiple rearrangements present in the same cells of the tumor focus. Using the tissue block that was used to construct the TMA with the QD technology, we were able to visualize the *TMPRSS2* and *NDRG1* rearrangements within the same nucleus (Figure 3). Interestingly, all cases with multiple rearrangements are characterized by *ERG* rearrangement through insertion. Using the next generation RNA sequencing, we have identified other examples of non-ETS rearrangements occurring concurrently with ETS rearrangements<sup>26</sup> (Pflueger and Rubin, unpublished observations). In these cases, the rearrangements do not appear to be recurrent but restricted to the individual case ('private events'). Some of these fusions may only occur in rare subclones of tumor cells unlike the common ETS rearrangements making them harder to detect by FISH or other *in situ* methods. Future studies will be required to determine whether these secondary rearrangements (both ETS and non-ETS) act in a synergistic manner with the primary molecular events to confer tumor growth advantage or simple represent passenger events. From the DNA sequencing of prostate cancer (Berger *et al*, unpublished data), we are also observing a multitude of other molecular muta-

tions that may also fit into a spectrum between passenger events and driver events. Taken together, the complexity of mutations and rearrangements should provide insight into prostate cancer disease progression. Other translocation tumors such as myeloma have been shown to harbor secondary translocations.<sup>27</sup>

The incidence of ETS rearrangement found in this study is in agreement with prior studies.<sup>7,15</sup> We confirmed *SLC45A3* as the second most common 5' gene partner, with a 12% rearrangement frequency in this cohort, similar to the 10% *SLC45A3* rearrangement frequency observed in a large cohort ( $n = 553$ ) from Berlin, Germany.

Many investigators have previously reported that when the *ERG* rearrangements occur, all of the tumor cells within a nodule show the alteration<sup>5,17</sup>; this suggests that this is either an early event or possibly an event that covers a growth advantage to the other tumor cells. We have also recently demonstrated this by immunohistochemistry using antibodies specific for the *ERG* rearrangement.<sup>28</sup> In the current study, we found cases showing intrafocal heterogeneity (ie both rearranged and non-rearranged nuclei in the same cancer focus). We also found cases where the same gene rearrangement showed both types of rearrangement mechanisms (ie rearrangement through insertion and deletion) within the same focus (Figure 5). These findings were seen in both ETS gene rearrangements and rearrangements of the 5' partners. Accumulating data suggest that the *TMPRSS2-ERG* fusion is an early molecular event based on the presence of the rearrangement in high-grade PIN, animal model data, and recent data from Attard *et al*,<sup>13</sup> showing that the circulating tumor cells either all have the ETS rearrangement or not. In the later study, they showed that other molecular alterations such as *PTEN* loss are only seen in a subset of the circulating tumor cells.

There is emerging data suggesting a functional role of ETS rearranged prostate cancer. However, some areas of clarification are needed. *In vitro* studies differ in terms of ETS role in cell proliferation. It has been widely shown that overexpression of *ERG*,<sup>29–31</sup> *ETV1*,<sup>32</sup> or *ETV5* leads to an increase in cell invasion but not proliferation. Recent studies

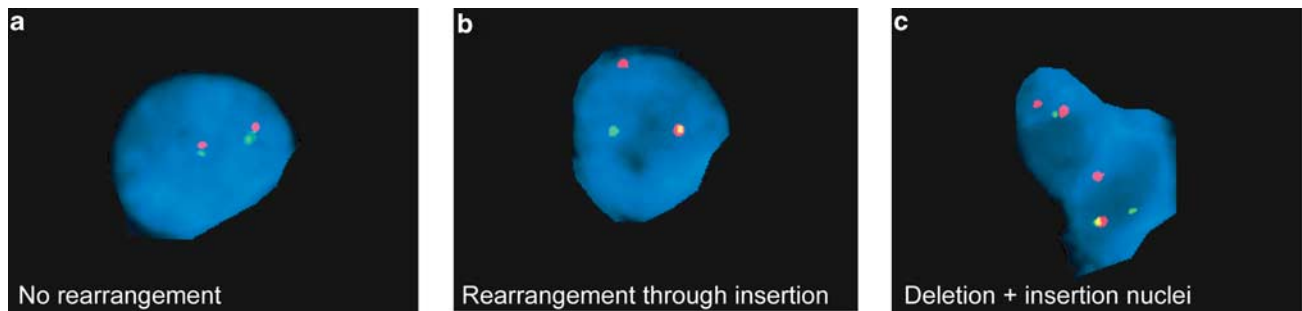


**Figure 5** Representative example of intrafocal heterogeneity with both *ERG* rearrangement negative (a) and rearrangement positive (b) nuclei within the same focus. We also found cases showing intrafocal heterogeneity regarding rearrangement mechanisms. Top nucleus rearranged through deletion and bottom nucleus through insertion (c).

have shown that inducing expression of ETS (ETV1 or ERG) leads to mouse PIN.<sup>29,30,32</sup> Other studies have shown that ERG overexpression does not lead to high-grade PIN in mice but can lead to aggressive adenocarcinoma if in combination with other genetic lesions (eg PTEN loss or AKT activation).<sup>33–35</sup> Subtle differences between the different mouse models may explain the discrepancies in the observations. Genetic analyses do not show an increase in genomic instability based on ETS rearrangement status. However, the specific types of genomic lesions do differ between rearrangement positive and negative cancers.<sup>36</sup> Thus, there is overwhelming data showing that ETS rearranged prostate cancer are phenotypically and molecularly different from prostate cancers lacking ETS gene rearrangements and that they may constitute a distinct subclass of prostate cancer.

The clinical implications of having a *TMPRSS2-ERG* fusion prostate cancer are still controversial.<sup>37</sup> Prostate cancer specific fusions are still helpful in the diagnosis of prostate cancer as they are highly cancer specific. In addition, similar to PCA3,<sup>38</sup> the *TMPRSS2-ERG* fusion can be detected in urine when present in the prostate gland. Hessels *et al*<sup>39</sup> and Laxman *et al*<sup>40</sup> both showed that multiplexed post-DRE urine assays searching for *TMPRSS2-ERG* fusion transcripts had high specificity and therefore may be successful as a prostate cancer screening tool. In both studies the sensitivity is low. The theoretical sensitivity is based on the frequency of the cancer-specific gene fusions. As demonstrated in the current study and other reports, a number of other, albeit less common cancer-specific gene fusions exist and would help improve the sensitivity of such an assay. Furthermore, the list of 5' fusion partners for *ERG* and other ETS family members is expanding.<sup>25,41</sup>

In summary, the frequencies of ETS rearrangement and 5' fusion partners in this study is similar to what has been previously reported. This is the first study to systematically examine multiple ETS rearrangement in multifocal prostate cancer. Our results demonstrate an additional level of complexity concerning the distribution of gene rearrangements in prostate cancer. This is exemplified by our observation that multiple rearrangements can exist within

one prostate gland, within the same tumor focus, and can also occur within the same nucleus. These events need to be further investigated to determine biological or clinical implications.

#### ACKNOWLEDGEMENTS

We thank Dr Arul Chinnaiyan for providing additional BAC clones and Dr Sven Perner for evaluating the cases for the TMA construction and assisting with parts of the FISH assessments. Dr David Rickman for helpful comments. Paul Chadwick at the Translational Research Program, Department of Pathology and Laboratory Medicine, Weill Cornell Medical College for TMA construction. Dr Raquel Esgueva for helping with parts of the FISH evaluations. This study was supported by NCI grant CA125612 (FD and MAR) and CA116337 (FD and MAR).

#### DISCLOSURE/CONFLICT OF INTEREST

F Demichelis and MA Rubin are listed as co-inventors on a patent filed by The University of Michigan and The Brigham and Women's Hospital covering the diagnostic and therapeutic fields for ETS fusions in prostate cancer. The diagnostic field has been licensed to Gen-Probe. Gen-Probe has not played a role in the design and conduct of the study, in the collection, analysis, or interpretation of the data, or in the preparation, review, or approval of the article. A Santa-Cruz, K Garsha, U Sathyanarayana, J Riley, S Yun, D Nagy, J Kosmeder and G Pestano are employed by Ventana a member of the Roche Group.

1. Ruijter ET, van de Kaa CA, Schalken JA, *et al*. Histological grade heterogeneity in multifocal prostate cancer. Biological and clinical implications. *J Pathol* 1996;180:295–299.
2. Arora R, Koch MO, Eble JN, *et al*. Heterogeneity of Gleason grade in multifocal adenocarcinoma of the prostate. *Cancer* 2004;100:2362–2366.
3. Greene DR, Wheeler TM, Egawa S, *et al*. A comparison of the morphological features of cancer arising in the transition zone and in the peripheral zone of the prostate. *J Urol* 1991;146:1069–1076.
4. Perner S, Svensson MA, Hossain RR, *et al*. ERG rearrangement metastasis patterns in locally advanced prostate cancer. *Urology* 2010;75:762–767.
5. Perner S, Mosquera JM, Demichelis F, *et al*. *TMPRSS2-ERG* fusion prostate cancer: an early molecular event associated with invasion. *Am J Surg Pathol* 2007;31:882–888.
6. Kumar-Sinha C, Tomlins SA, Chinnaiyan AM. Recurrent gene fusions in prostate cancer. *Nat Rev Cancer* 2008;8:497–511.
7. Mosquera JM, Mehra R, Regan MM, *et al*. Prevalence of *TMPRSS2-ERG* fusion prostate cancer among men undergoing prostate biopsy in the United States. *Clin Cancer Res* 2009;15:4706–4711.

8. Barry M, Perner S, Demichelis F, *et al*. TMPRSS2-ERG fusion heterogeneity in multifocal prostate cancer: clinical and biologic implications. *Urology* 2007;70:630–633.
9. Mehra R, Han B, Tomlins SA, *et al*. Heterogeneity of TMPRSS2 gene rearrangements in multifocal prostate adenocarcinoma: molecular evidence for an independent group of diseases. *Cancer Res* 2007;67:7991–7995.
10. Clark J, Attard G, Jhavar S, *et al*. Complex patterns of ETS gene alteration arise during cancer development in the human prostate. *Oncogene* 2008;27:1993–2003.
11. Mehra R, Tomlins SA, Yu J, *et al*. Characterization of TMPRSS2-ETS gene aberrations in androgen-independent metastatic prostate cancer. *Cancer Res* 2008;68:3584–3590.
12. Liu W, Laitinen S, Khan S, *et al*. Copy number analysis indicates monoclonal origin of lethal metastatic prostate cancer. *Nat Med* 2009;15:559–565.
13. Attard G, Swennenhuis JF, Olmos D, *et al*. Characterization of ERG, AR and PTEN gene status in circulating tumor cells from patients with castration-resistant prostate cancer. *Cancer Res* 2009;69:2912–2918.
14. Tomlins SA, Rhodes DR, Perner S, *et al*. Recurrent fusion of TMPRSS2 and ETS transcription factor genes in prostate cancer. *Science* 2005;310:644–648.
15. Han B, Mehra R, Dhanasekaran SM, *et al*. A fluorescence *in situ* hybridization screen for E26 transformation-specific aberrations: identification of DDX5-ETV4 fusion protein in prostate cancer. *Cancer Res* 2008;68:7629–7637.
16. Cheng L, Song SY, Pretlow TG, *et al*. Evidence of independent origin of multiple tumors from patients with prostate cancer. *J Natl Cancer Inst* 1998;90:233–237.
17. Perner S, Demichelis F, Beroukhir R, *et al*. TMPRSS2:ERG fusion-associated deletions provide insight into the heterogeneity of prostate cancer. *Cancer Res* 2006;66:8337–8341.
18. Feinberg AP, Vogelstein B. A technique for radiolabeling DNA restriction endonuclease fragments to high specific activity. *Anal Biochem* 1983;132:6–13.
19. Chan WC, Nie S. Quantum dot bioconjugates for ultrasensitive nonisotopic detection. *Science* 1998;281:2016–2018.
20. Macville MV, Van der Laak JA, Speel EJ, *et al*. Spectral imaging of multi-color chromogenic dyes in pathological specimens. *Anal Cell Pathol* 2001;22:133–142.
21. Malik Z, Dishi M, Garini Y. Fourier transform multipixel spectroscopy and spectral imaging of protoporphyrin in single melanoma cells. *Photochem Photobiol* 1996;63:608–614.
22. Schrock E, du Manoir S, Veldman T, *et al*. Multicolor spectral karyotyping of human chromosomes. *Science* 1996;273:494–497.
23. Veldman T, Vignon C, Schrock E, *et al*. Hidden chromosome abnormalities in haematological malignancies detected by multicolour spectral karyotyping. *Nat Genet* 1997;15:406–410.
24. Garini Y, Young IT, McNamara G. Spectral imaging: principles and applications. *Cytometry A* 2006;69:735–747.
25. Pflueger D, Rickman DS, Sboner A, *et al*. N-myc downstream regulated gene 1 (NDRG1) is fused to ERG in prostate cancer. *Neoplasia* 2009;11:804–811.
26. Palanisamy N, Ateeq B, Kalyana-Sundaram S, *et al*. Rearrangements of the RAF kinase pathway in prostate cancer, gastric cancer and melanoma. *Nat Med* 2010;16:793–798.
27. Bergsagel PL, Kuehl WM. Chromosome translocations in multiple myeloma. *Oncogene* 2001;20:5611–5622.
28. Park K, Tomlins S, Mudaliar KM, *et al*. Antibody-based detection of ERG rearrangement-positive prostate cancer. *Neoplasia* 2010;12:590–598.
29. Tomlins SA, Laxman B, Varambally S, *et al*. Role of the TMPRSS2-ERG gene fusion in prostate cancer. *Neoplasia* 2008;10:177–188.
30. Klezovitch O, Risk M, Coleman I, *et al*. A causal role for ERG in neoplastic transformation of prostate epithelium. *Proc Natl Acad Sci USA* 2008;105:2105–2110.
31. Wang J, Cai Y, Yu W, *et al*. Pleiotropic biological activities of alternatively spliced TMPRSS2/ERG fusion gene transcripts. *Cancer Res* 2008;68:8516–8524.
32. Tomlins SA, Laxman B, Dhanasekaran SM, *et al*. Distinct classes of chromosomal rearrangements create oncogenic ETS gene fusions in prostate cancer. *Nature* 2007;448:595–599.
33. Carver BS, Tran J, Gopalan A, *et al*. Aberrant ERG expression cooperates with loss of PTEN to promote cancer progression in the prostate. *Nat Genet* 2009;41:619–624.
34. King JC, Xu J, Wongvipat J, *et al*. Cooperativity of TMPRSS2-ERG with PI3-kinase pathway activation in prostate oncogenesis. *Nat Genet* 2009;41:524–526.
35. Zong Y, Xin L, Goldstein AS, *et al*. ETS family transcription factors collaborate with alternative signaling pathways to induce carcinoma from adult murine prostate cells. *Proc Natl Acad Sci USA* 2009;106:12465–12470.
36. Demichelis F, Setlur SR, Beroukhir R, *et al*. Distinct genomic aberrations associated with ERG rearranged prostate cancer. *Genes Chromosomes Cancer* 2009;48:366–380.
37. Tomlins SA, Bjartell A, Chinnaiyan AM, *et al*. ETS gene fusions in prostate cancer: from discovery to daily clinical practice. *Eur Urol* 2009;56:275–286.
38. Groskopf J, Aubin SM, Deras IL, *et al*. APTIMA PCA3molecular urine test: development of a method to aid in the diagnosis of prostate cancer. *Clin Chem* 2006;52:1089–1095.
39. Hessels D, Smit FP, Verhaegh GW, *et al*. Detection of TMPRSS2-ERG fusion transcripts and prostate cancer antigen 3 in urinary sediments may improve diagnosis of prostate cancer. *Clin Cancer Res* 2007;13:5103–5108.
40. Laxman B, Morris DS, Yu J, *et al*. A first-generation multiplex biomarker analysis of urine for the early detection of prostate cancer. *Cancer Res* 2008;68:645–649.
41. Maher CA, Palanisamy N, Brenner JC, *et al*. Chimeric transcript discovery by paired-end transcriptome sequencing. *Proc Natl Acad Sci USA* 2009;106:12353–12358.



This work is licensed under the Creative Commons Attribution-NonCommercial-No Derivative Works 3.0 Unported License. To view a copy of this license, visit <http://creativecommons.org/licenses/by-nc-nd/3.0/>